LASER DOPPLER VIBROMETRY FOR MACHINING DYNAMICS ANALYSIS

Michael Gomez[1], Emma Betters[1], Jerome Eichenberger[2], Thomas S. Delio[3], and Tony L. Schmitz[1]
[1]Department of Mechanical, Aerospace, and Biomedical Engineering, University of Tennessee, Knoxville, TN, USA
[2]Polytec, Inc., Irvine, CA, USA
[3]Manufacturing Laboratories Inc., Las Vegas, NV, USA

INTRODUCTION

Optimizing machining operations in discrete part production remains a critical step in the realization of productivity enhancement, yield improvement, reject rate reduction, improved surface finish, increased part accuracy, and reduced tool wear. Production environments typically rely on the skill and experience of process planners and machinists to select tools and cutting conditions. Handbooks and tool catalogs are often applied as a resource, but these usually supply conservative cutting conditions that may reduce productivity due to suboptimal use of machining capability [1-3]. Because the vibration level depends on the relationship between the tooth passing frequency (i.e., the product of the rotating speed and number of teeth) and the system natural frequencies (e.g., the first bending mode of the endmill), spindle speed and, therefore, cutting speed selection is critical [1-2]. Due to these complications, an important ongoing research area is establishing effective methods for optimizing machining operations.

In this paper, in-process laser Doppler vibrometer measurements are used to assess stability and tool wear for milling a low carbon steel alloy. A comparison of the wear rate for stable resonant and non-resonant cutting speeds is also provided and correlated to the measured vibration signals.

LASER VIBROMETRY

The use of laser Doppler vibrometers (LDVs) as vibration transducers for machining dynamics analysis is common [4-9]. This provides noncontact measurement with high accuracy from a distance [5, 10-11]. LDVs measure motion using the Doppler frequency shift of the laser light reflected from the moving target surface [10].

The LDV used in this study was a Polytec OFV 5000 controller/OFV 534 laser head, which was able to simultaneously measure displacement and velocity. This enabled Poincaré maps to be generated that describe machining behavior graphically. The velocity decoder VD-09 and displacement decoder DD-900 provided ranges from 5 mm/s/V to 1 m/s/V and 50 nm/V to 5 mm/V [10]. A tracking filter was used due to "low backscattered light" [11]. The speckled nature of laser light on a diffuse surface can lead to brief moments when the amount of backscattered light is reduced. The tracking filter bridges these intervals using a phase-locked loop to provide clean data traces [10-11].

EXPERIMENTAL SETUP

The experimental setup for milling stability verification and tool wear is shown in Fig 1. The flexure and tool point dynamics were measured by impact testing, where an instrumented hammer (PCB 086C04) was used to excite the structure and the response was measured using a low mass accelerometer (PCB 352C23).

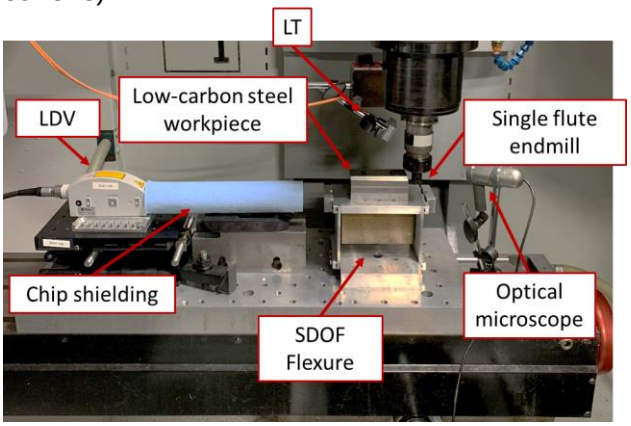

FIGURE 1. Experimental setup for milling stability and tool wear testing.

Cutting tests were performed on a Haas TM-1 computer numerically-controlled (CNC) vertical milling machine. A low carbon steel alloy workpiece was mounted on a parallelogram, leaf-type flexure. The compliant direction for the flexure was oriented parallel to the machine's x (feed) direction; see Fig. 2. A single flute, 19.05 mm diameter, 30 deg helix endmill was used to perform machining passes at a 4.76 mm radial depth of cut (25% radial immersion) and 2 mm axial depth of cut. Once-per-tooth sampling was achieved using a laser tachometer (LT), where a reflective target was attached to the rotating tool holder. In situ vibration signals were collected using

the LDV. An optical microscope (DinoLite Pro-AM4137) was used to record the flank wear width for the cutting edge (FWW) at regular intervals during the tool wear testing.

First, milling stability was predicted using a time domain simulation and then verified by the measured vibration signals obtained during the machining process. For the purposes of simulation, the tool was considered rigid with respect to the flexure. This assumption is confirmed by the frequency response function (FRF) measurements shown in Fig. 3 and the modal parameters listed in Table 1. Second, tests were carried out to monitor tool wear progression for resonant and non-resonant cutting speeds.

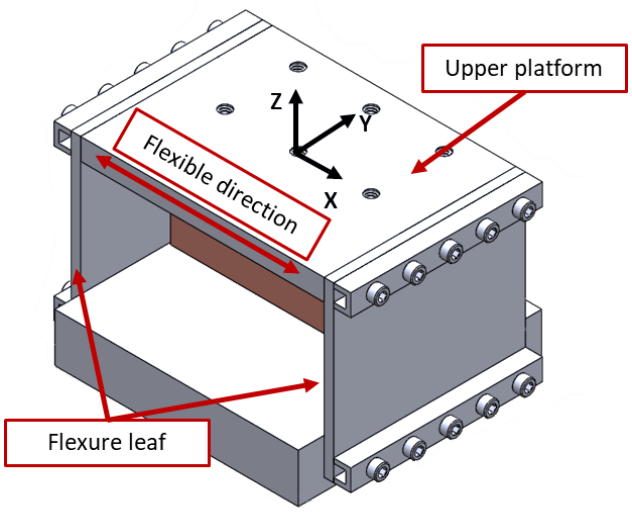

FIGURE 2. Single degree of freedom flexure.

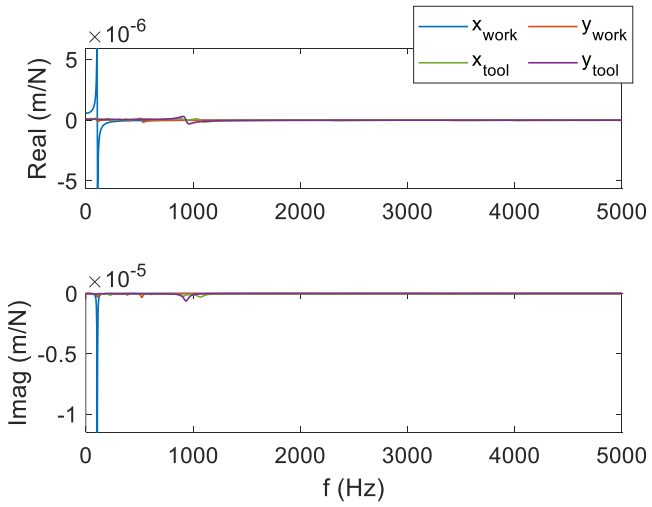

FIGURE 3. Measured FRFs of the tool and workpiece for the stability and tool wear testing.

TABLE 1. Modal parameters for milling simulations (mass, m, stiffness, k, and damping coefficient, c).

Direction	m (kg)	k (N/m)	c (N-s/m)
Tool			
x (feed)	0.88	5.0×10^7	1330
y	0.88	5.0×10^7	1330
Workpiece			
x (feed)	3.89	1.74×10^6	125
y	0.88	5.0×10^7	1330

RESULTS

Stability

A time domain simulation was used to predict the forces and displacements during milling. It was based on the "Regenerative Force, Dynamic Deflection" model described by Smith and Tlusty [12]. The simulation proceeded as follows.

- The instantaneous chip thickness was determined using the vibration of the previous and current teeth and commanded chip thickness at the selected tooth angle.
- The cutting force components were calculated as the product of the chip width (axial depth), chip thickness, and cutting force coefficients.
- The force was used to find the new displacement by modified Euler (numerical) integration of the second order, time delay differential equations of motion.
- The tooth angle was incremented and the process was repeated.

The simulation accounts for the non-linearity that can occur if the tooth leaves the cut due to large vibrations. It can also accommodate cutter teeth runout, variable teeth spacing, and variable helix angles [1, 12].

Stability testing was completed using the Fig. 1 setup. Workpiece (flexure) displacement and velocity predictions were generated using the time domain simulation and compared to measured signals. Stability lobe validation was achieved by selecting stable and unstable combinations of spindle speed and axial depth of cut and evaluating the behavior.

Simulations were completed over a grid of equally spaced points in spindle speed and axial depth. To establish stability, the workpiece x direction displacement and velocity signals were sampled once-per-tooth (i.e., at the tooth passing frequency) [8-9]. This periodic sampling approach was used to determine if the milling response was synchronous with the tooth passing frequency or not. Synchronous motion indicates stable behaviour, while anything else indicates unstable behaviour.

To automatically determine stability, a metric was applied where the absolute values of the differences in pairs of sequentially sampled points was summed

and then normalized to the number of sampled points. For forced (synchronous) vibration, the points repeat so this metric is ideally zero. For other behaviors, it is greater than zero [9]. Figure 4 shows a stability map produced using this metric. The dots indicate stable (forced vibration) performance. The circles identify period-2 bifurcations, where the motion repeats every other tooth passage (also referred to as period doubling bifurcations). The open area indicates all other bifurcation types, including secondary Hopf and higher-order period-n bifurcations (n = 3, 4, …). In Fig. 5, the stable behaviour (white zone) is separated from other bifurcation types by the stability limit (solid line). The test points are also identified.

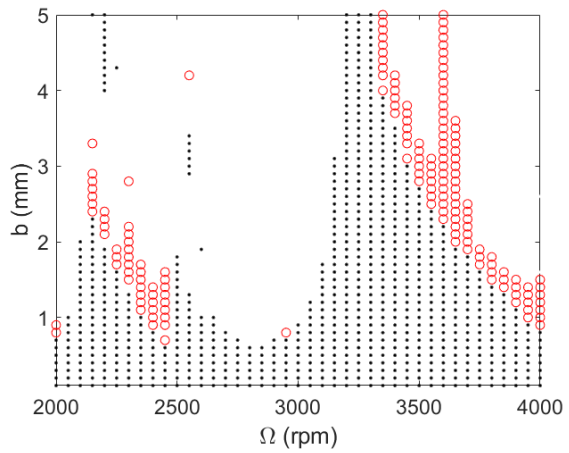

FIGURE 4. Predicted stability map for down milling at a 4.76 mm radial depth (25% radial immersion) and 150 μm/tooth feed using the Table 1 dynamics. The grid contains 2000 points.

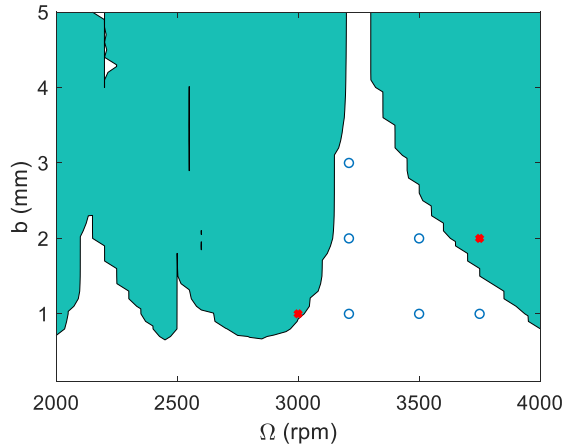

FIGURE 5. Predicted stability map with test points. Open circles were stable and filled were unstable.

The once-per-tooth sampling strategy was also used to produce Poincaré maps, where the time synchronized LDV displacement and velocity are plotted in the phase plane. The results of this approach are presented in Figs. 6-8 for the 2 mm axial depth of cut trials.

Figures 6 and 7 demonstrate stable cuts, where the once-per-tooth samples repeat. Note the change in scale between the two figures; the workpiece motion at resonance (i.e., where the tooth passing frequency is near the flexure's natural frequency) is much larger than the motion when not at resonance. However, both exhibit only a single grouping of points in the Poincaré map, which indicates forced vibration and stable operation.

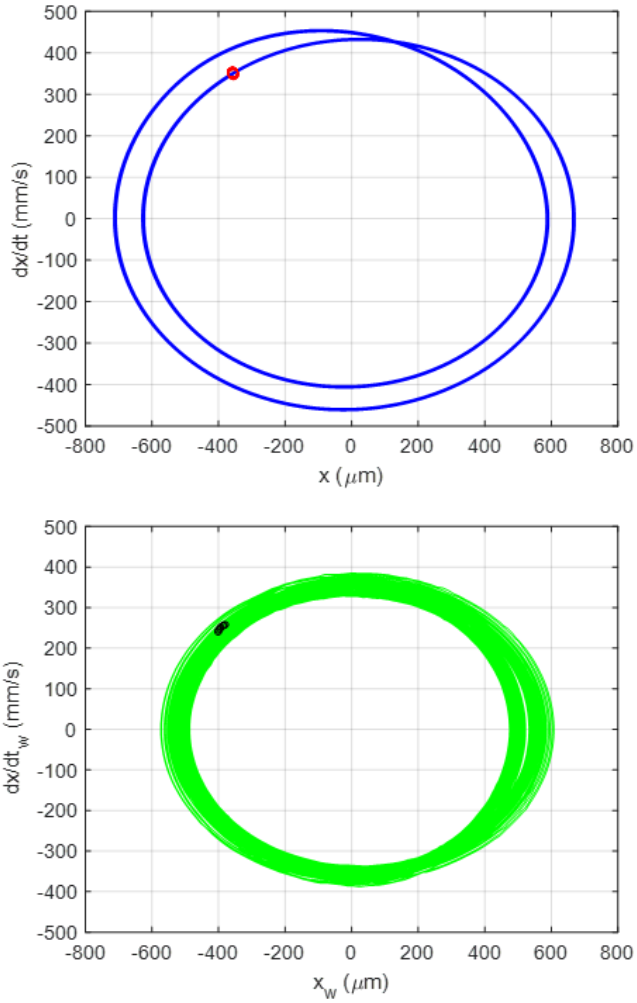

FIGURE 6. Poincaré maps for stable cutting at resonance {3210 rpm, 2 mm}. (Top) predicted. (Bottom) measured.

Figure 8, on the other hand, does not show a single grouping of periodically sampled points. Rather, an elliptical distribution is observed. This means that the behaviour changes from one tooth passage to the next. The elliptical shape is indicative

of a secondary Hopf bifurcation, or classic self-excited vibration caused by regeneration of the machined surface. In other words, the chip thickness for the current tooth depends on the commanded chip thickness (defined by the feed per tooth and cutter angle), the vibration state now, and the surface left behind by the previous tooth.

FIGURE 7. Poincaré maps for stable cutting away from resonance {3500 rpm, 2 mm}. (Top) predicted. (Bottom) measured.

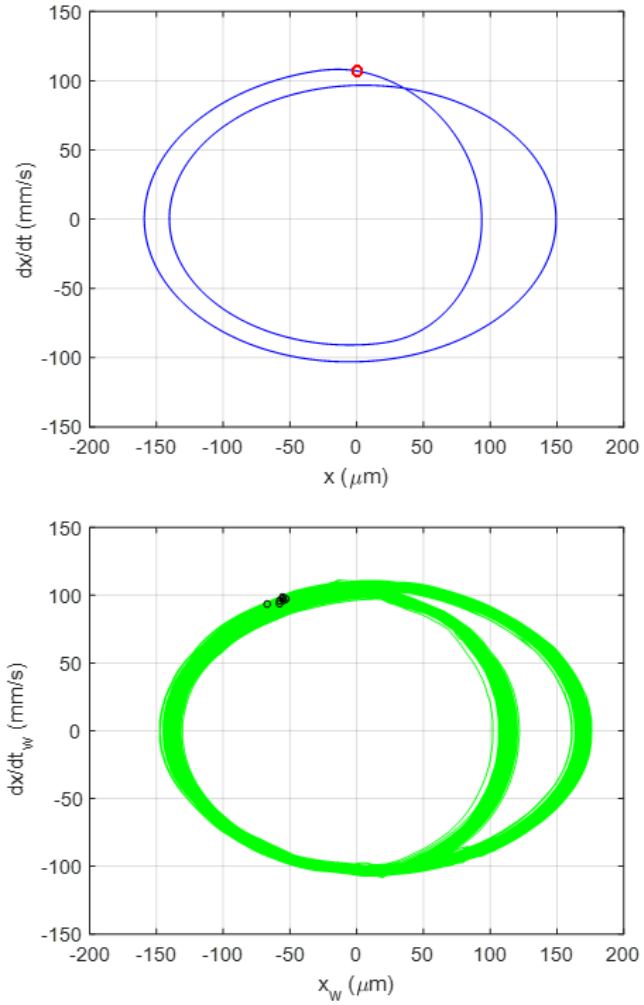

Tool wear

Tool wear tests were completed at two cutting speeds, with all other conditions held constant. The first set of tests was conducted at a stable cutting speed where the first harmonic of the tooth passing frequency matched the flexure's natural frequency (resonance). The second set was completed at a higher cutting speed (the first harmonic was above the flexure's natural frequency).

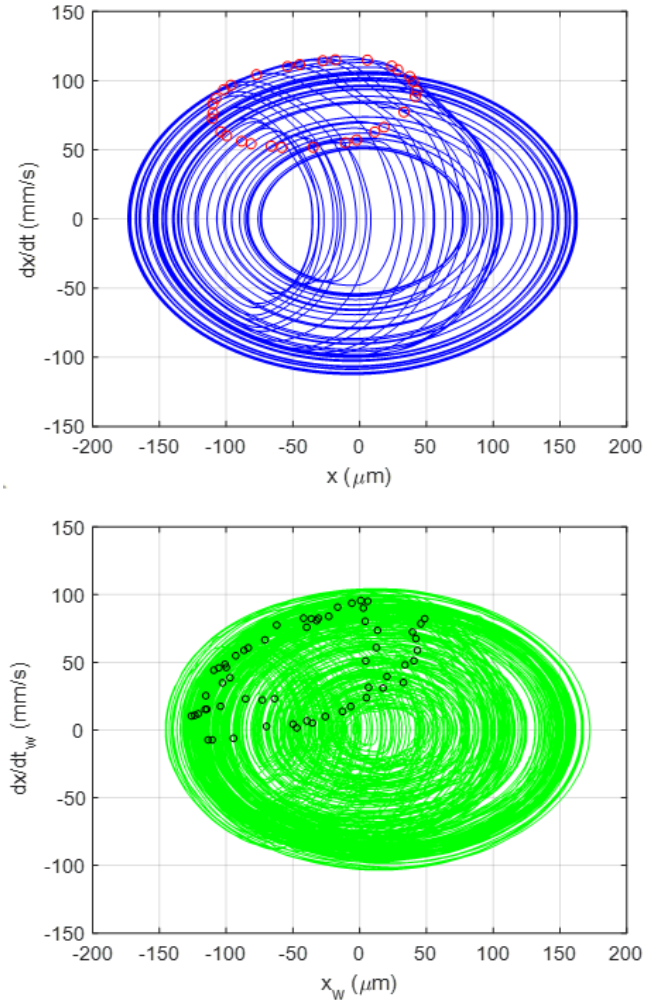

FIGURE 8. Poincaré maps for unstable cutting {3750 rpm, 2 mm}. (Top) predicted. (Bottom) measured.

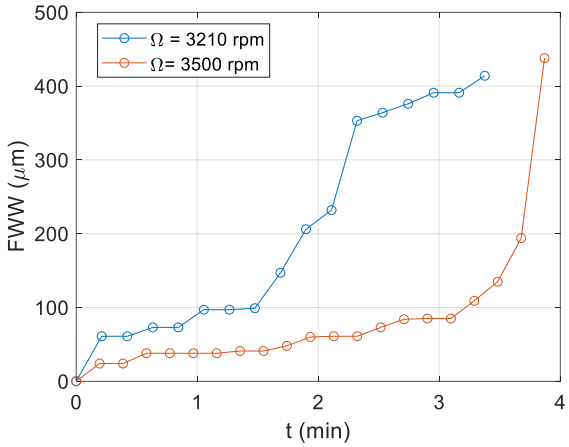

FIGURE 9. Maximum FWW progression as a function of time for all trials.

After each down milling pass, the FWW was measured. The maximum FWW was recorded for each pass and the results are summarized in Fig. 9. The volume per cut was approximately 967 mm^3 (101.6 mm × 2.0 mm × 4.8 mm). As expected, the FWW grows with increasing cutting time/volume for both cutting speeds. The images used to construct Fig. 9 are provided in Fig. 10. The progression of the flank wear is provided with FWW measurement values at four cutting time increments, t_c = {0, 1, 2, and 4} min.

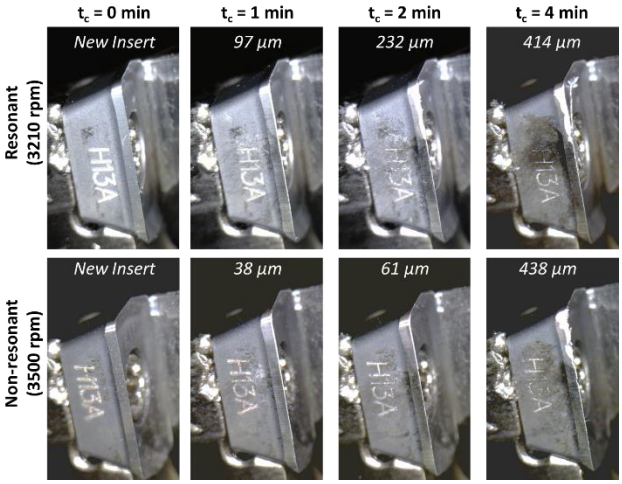

FIGURE 10. FWW progression. Images collected using the on-machine digital microscope. In the images, the rake face is on the right and the flank face is shown. The numerical FWW values are included at four cutting time intervals.

The interesting result from Fig. 9 is that a higher wear rate is obtained for the lower cutting speed. Specifically, the cutting tests at 3210 rpm reached a FWW of 300 µm (a traditional limiting value for carbide) in 2.2 min, while the 3500 rpm tests required 3.7 min. This is an unexpected result since the traditional Taylor tool life model relates the tool life to cutting speed using a simple power law; see Eq. 1, where V_c is the cutting speed, T is the tool life, and n and C are parameters that depend on the cutting conditions, work material, tool material and coating, and the tool life criterion [2]. This empirical relationship predicts that the higher cutting speed should yield a lower tool life. Clearly, the vibration magnitude difference between the resonant (3210 rpm) and non-resonant (3500 rpm) conditions also plays a role.

$$V_c T^n = C \quad (1)$$

To examine the tool life results further, the displacement and velocity levels were compared for the two tests. Figure 11 displays the synchronized displacement and velocity measured by the LDV for 3210 rpm. Figure 12 shows the results for 3500 rpm. It is seen that the vibration levels are approximately four times higher for the resonant condition at 3210 rpm. It is proposed that the increased magnitude caused the higher wear rate. Figures 11 and 12 both include displacement and velocity signals for new and worn cutting edges. It is seen that both signals indicate tool wear by the increase in magnitude.

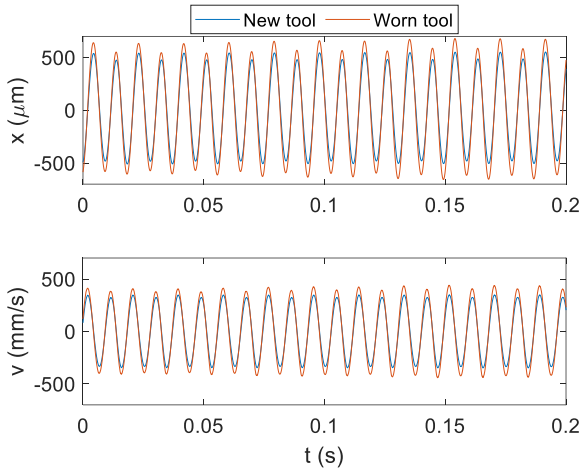

FIGURE 11. Stable, 3210 rpm cut results for x (feed) direction displacement (top) and velocity (bottom) for a new and worn tool insert.

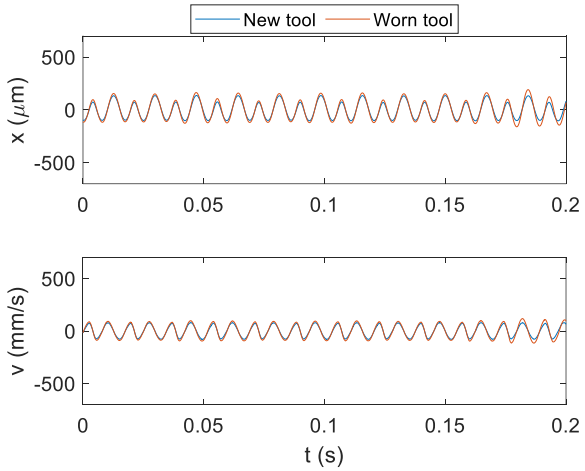

FIGURE 12. Stable, 3500 rpm cut for x (feed) direction displacement (top) and velocity (bottom) for a new and worn tool insert.

CONCLUSIONS

This paper presented stability and tool life studies using laser Doppler vibrometry as the process signal. It was shown that periodic sampling of the measured displacement and velocity signals could be used to

identify stable and unstable cutting conditions. Additionally, good agreement was obtained between predicted and measured behaviour.

During tool life testing, it was observed that the tool life increased with a higher cutting speed. This counter-intuitive behavior was attributed to a much larger vibration magnitude for the lower cutting speed. This higher magnitude was obtained because the lower cutting speed corresponded to a tooth passing frequency whose first harmonic matched the natural frequency for the flexure-based machining setup (resonant conditions).

In future work, additional tests will be performed to verify the preliminary results obtained in this study. The FWW progression with cutting time will be recorded for additional cutting speeds and the displacement and velocity will be measured to demonstrate that these signals can be used to indicate process health (stability and tool wear).

REFERENCES

[1] Schmitz, T.L. and Smith, K.S., 2009, Machining Dynamics: Frequency Response to Improved Productivity, Springer, New York, NY.

[2] Altintas, Y., 2012, Manufacturing Automation: Metal Cutting Mechanics, Machine Tool Vibrations, and CNC Design, Cambridge University Press.

[3] Pohokar, N.S. and Bhuyar, L.B., 2012, Optimization of tools for CNC machine: An explanation and overview, International Journal of Scientific & Engineering Research, 3/12: 1-9.

[4] Bediz, B., Uttara, K., Schmitz, T.L., Ozdoganlar, O.B., 2012, Modeling and experimentation for three-dimensional dynamics of endmills, International Journal of Machine Tools & Manufacture, 53/1: 39-50.

[5] Ozdoganlar, O.B., Hanshe, B.D., Carne, T.G., 2005, Experimental modal analysis for micromechanical systems, Experimental Mechanics, 46/6: 498-506.

[6] Özşahin, O., Budak, E., Özgüven, H.N., 2011, Investigating dynamics of machine tool spindles under operational conditions, Advanced Materials Research, 223/1: 610-621.

[7] Honeycutt, A., Schmitz, T.L., 2016, Experimental validation of period-n bifurcations in milling, Procedia Manufacturing, 5: 362-374.

[8] Honeycutt, A., Schmitz, T.L., 2016, A new metric for automated stability identification in time domain milling simulation, Journal of Manufacturing Science and Engineering, 138/7: 075401.

[9] Honeycutt, A., Schmitz, T.L., 2017, Milling stability interrogation by subharmonic sampling, Journal of Manufacturing Science and Engineering, 139/4: 041009.

[10] Polytec, 2016, OFV-5000 vibrometer controller datasheet, 1-12.

[11] Chan, A., 2011, Vocal fold vibration measurements using laser Doppler vibrometry, McGill University Master's Thesis, 3: 16-20.

[12] Smith, K.S. and Tlusty, J., 1991, An overview of modelling and simulation of the milling process, Journal of Engineering for Industry, 116/2: 169-175.